

University of Groningen

The toroidal moment in condensed-matter physics and its relation to the magnetoelectric effect

Spaldin, Nicola A.; Fiebig, Manfred; Mostovoy, Maxim

Published in:
Journal of Physics-Condensed Matter

DOI:
[10.1088/0953-8984/20/43/434203](https://doi.org/10.1088/0953-8984/20/43/434203)

IMPORTANT NOTE: You are advised to consult the publisher's version (publisher's PDF) if you wish to cite from it. Please check the document version below.

Document Version
Publisher's PDF, also known as Version of record

Publication date:
2008

[Link to publication in University of Groningen/UMCG research database](#)

Citation for published version (APA):

Spaldin, N. A., Fiebig, M., & Mostovoy, M. (2008). The toroidal moment in condensed-matter physics and its relation to the magnetoelectric effect. *Journal of Physics-Condensed Matter*, 20(43), [434203].
<https://doi.org/10.1088/0953-8984/20/43/434203>

Copyright

Other than for strictly personal use, it is not permitted to download or to forward/distribute the text or part of it without the consent of the author(s) and/or copyright holder(s), unless the work is under an open content license (like Creative Commons).

The publication may also be distributed here under the terms of Article 25fa of the Dutch Copyright Act, indicated by the "Taverne" license. More information can be found on the University of Groningen website: <https://www.rug.nl/library/open-access/self-archiving-pure/taverne-amendment>.

Take-down policy

If you believe that this document breaches copyright please contact us providing details, and we will remove access to the work immediately and investigate your claim.

Downloaded from the University of Groningen/UMCG research database (Pure): <http://www.rug.nl/research/portal>. For technical reasons the number of authors shown on this cover page is limited to 10 maximum.

The toroidal moment in condensed-matter physics and its relation to the magnetoelectric effect*

Nicola A Spaldin¹, Manfred Fiebig² and Maxim Mostovoy³

¹ Materials Department, University of California, Santa Barbara, CA 93106-5050, USA

² HISKP, Universität Bonn, Nussallee 14-16, 53115 Bonn, Germany

³ Zernike Institute for Advanced Materials, University of Groningen, 9747 AG Groningen, The Netherlands

E-mail: nicola@mrl.ucsb.edu, fiebig@hiskp.uni-bonn.de and m.mostovoy@rug.nl

Received 17 April 2008, in final form 4 June 2008

Published 9 October 2008

Online at stacks.iop.org/JPhysCM/20/434203

Abstract

The concept of toroidal moments in condensed-matter physics and their long-range ordering in a so-called ferrotoroidic state is reviewed. We show that ferrotoroidicity as a form of primary ferroic order can be understood both from microscopic (multipole expansion) and macroscopic (symmetry-based expansion of the free energy) points of view. The definition of the local toroidal moment and its transformation properties under the space-inversion and time reversal operations are highlighted and the extension to periodic bulk systems is discussed. Particular attention is paid to the relationship between the toroidal moment and the antisymmetric magnetoelectric effect and to limitations of the magnetoelectric response in ferrotoroidic systems and ferroic materials in general. Experimental access to the ferrotoroidic state by magnetoelectric susceptibility measurements, x-ray diffraction and optical techniques or direct measurement of the bulk toroidization is discussed. We outline the pertinent questions that should be clarified for continued advancement of the field and mention some potential applications of ferrotoroidic materials.

1. Introduction

The search for novel states of matter and new types of order is one of the most exciting and fundamental aspects of modern condensed-matter physics. Anyon gases in fractional quantum Hall systems, d-wave electron pairing in high-temperature superconductors and electron nematic phases in transitional metal oxides have recently enriched our understanding of the complex ways in which strongly correlated matter can organize itself [1, 2]. Some ordered states escape detection and remain hidden for a long time, as their nature can only be revealed by a purposely designed experimental probe. For example, while ferromagnetism has been known to mankind since time immemorial, antiferromagnetism was discovered only relatively recently despite the fact that antiferromagnets are far more common than ferromagnets in nature.

The purpose of this article is to summarize our current understanding of such an elusive type of long-range order: *ferrotoroidicity*. By analogy with the spontaneous alignment of magnetic dipole moments in ferromagnets, ferrotoroidics are defined to have a spontaneous alignment of *toroidal moments* [3–5], of which a classical example is a solenoid that is bent into a torus [6]. As shown in figure 1 the current induces a circular magnetic field inside the solenoid, giving rise to a toroidal moment perpendicular to the magnetic field. The quantum-mechanical equivalent can be generated by certain spin orderings, such as head-to-tail arrangements of spins, or by persistent orbital currents. A ferrotoroidic state can then be visualized as an array of spin vortices, each of the size of one unit cell, which is a magnetic analogue of the electronic flux states discussed in the context of quantum Hall systems and high-temperature superconductors [6, 7].

In this paper we describe the existing state of knowledge of toroidal moments and toroidal ordering in the solid state.

* All authors contributed equally to this work.

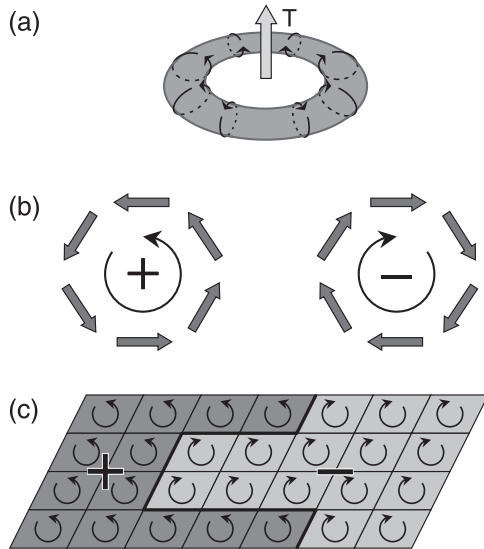


Figure 1. Toroidal moment, magnetoelectric effect and ferrotoroidic order. (a) Ring-shaped solenoid with electric-current loops as classical example for a toroidal moment. (b) A head-to-tail arrangement of atomic magnetic moments is a quantum-mechanical example of a toroidal moment. The two vortices displayed correspond to opposite toroidal moments. (c) Sketch of a ferrotoroidic domain structure with curls in boxes representing unit cells with magnetic vortices as in (c).

The toroidal moment has long been discussed in the context of particle physics (see appendix A) and interest within the solid state community has recently increased drastically because of its relationship to the magnetoelectric effect and the consequent implications for the active field of multiferroics. The toroidal moment constitutes a fundamental building block both in an expansion of the free energy into contributions of different symmetry as well as in the multipole expansion of the electromagnetic vector potential. Nevertheless, its description is not contained in standard textbooks which has led to ambiguities and confusion in the field. We hope to rectify that here.

The remainder of this paper is organized as follows. In section 2 we introduce the concept of ferrotoroidic long-range order using general macroscopic symmetry considerations based on transformation properties of the order parameter under space-inversion and time reversal operations. The microscopic sources of such ferrotoroidic order are elucidated by considering the magnetic multipole expansion as well as the expansion of free energy in terms of gradients of an external magnetic field. The toroidal moment will emerge as a third type of vector order parameter describing the distribution of spins and electric currents in a system, in addition to the well-known magnetic and electric dipole. In section 3 the magnetoelectric effect is introduced phenomenologically as the coupling between the magnetic field and the electric polarization, and the electric field and the magnetization and the relation between ferrotoroidic order and the magnetoelectric effect will be elucidated. We show that the ferrotoroidic order parameter gives rise to antisymmetric contributions to the magnetoelectric effect, but not necessarily

vice versa. In section 4 the upper bound limiting the magnitude of the magnetoelectric coupling in toroidically ordered and disordered systems is discussed, and the limit imposed by thermodynamic stability is identified. We introduce simple microscopic mechanisms for magnetoelectric behaviour in which the magnitude of the magnetoelectric coefficient is determined by the geometric aspects of the superexchange interaction. In section 5 experimental techniques probing the peculiar symmetry of a ferrotoroidic state are reviewed. The magnetoelectric effect as well as gyrotropic and dichroic x-ray and optical effects are discussed and we show that nonlinear optical techniques are quite powerful in observing ferrotoroidic order and domains. In section 6 various issues related to the future practical merit of ferrotoroidics are highlighted. Ways for measuring and switching a ferrotoroidic state and the potential of ferrotoroidicity for magnetoelectric and data storage devices are discussed. We also speculate on the possible existence of antiferrotoroidic order. A concluding section follows in which some pertinent questions to be clarified for the continued advancement of the field are discussed. Note that Gaussian units are used throughout this article.

2. Macroscopic and microscopic derivations

2.1. Macroscopic motivation: symmetry expansion

2.1.1. Ferroic order. A hallmark of any ferroic state is the formation of domains, which are energetically degenerate regions of identical structure, that have different orientations of the ferroic order parameter [8]. An appropriate vector or tensor field can be used to induce an energy difference between states with different orientations of the order parameter. Such a field can therefore be used to switch domain states, which adopt the orientation with the lowest energy in the presence of the field. For example, in ferroelectric materials there is a contribution to the free energy of form $-P_{sp} \cdot E$, which causes domains with spontaneous polarization P_{sp} parallel to an electric field E to have lowest energy. An electric field of sufficient strength then transforms a sample into a uniformly polarized domain state with $P_{sp} \parallel E$ since this minimizes the free energy. More generally, any ferroic state is characterized by a macroscopic property \hat{O} corresponding to the order parameter (here P_{sp}) that can be switched by an external field \hat{A} (here E) because of a field-energy contribution

$$F_{ferro} = -\hat{O} \hat{A} \quad (1)$$

to the free energy. Any ferroic state obeying (1) is called *primary ferroic* because a single field \hat{A} is required to switch the domains. A ferroic state described by $F_{ferro} = -\hat{O}_{12} \hat{A}_1 \hat{A}_2$ is called *secondary ferroic* because two fields, \hat{A}_1 and \hat{A}_2 , are required to set the direction of the order parameter \hat{O}_{12} . The extension towards ferroics of even higher order is obvious. As an example, a state parametrized by $F_{biel} = -\epsilon_{ij} E_i E_j$, with $\hat{\epsilon}$ as the switchable order parameter is called *ferrobielectric*. A secondary ferroic state of high relevance for this paper is the *ferromagnetoelectric* state described by $F_{me} = -\alpha_{ij} E_i H_j$. However, note that for secondary or higher-order ferroics the


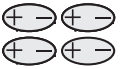
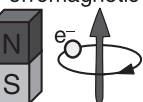
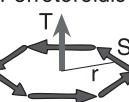
Time \ Space	Invariant	Change
Invariant	Ferroelastic 	Ferroelectric 
Change	Ferromagnetic 	Ferrotoroidic 

Figure 2. Forms of ferroic order and their transformation properties under the parity operations of spatial inversion and time reversal.

denomination as ferroic and the prefix ‘ferro’ are usually not applied.

2.1.2. Space–time symmetry. The primary ferroic states can be classified in terms of the spatial inversion and time reversal symmetry of their order parameter. As shown in figure 2 three established forms of primary ferroic order are known at present. Each of them transforms according to one of the representations of the space–time-inversion group. Ferroelectricity is characterized by a spontaneous polarization, a quantity that changes sign under spatial inversion but remaining invariant under time reversal. Ferromagnetism corresponds to a spontaneous magnetization changing sign under time reversal but remaining invariant under spatial inversion. Ferroelasticity is accompanied by a spontaneous strain for which both space-and time-inversion are symmetry operations.

The existence of a fourth state with a spontaneous order changing its sign upon application of space *or* time-inversion suggests itself. As is evident from figures 1(a) and (b), toroidal moments change sign not only upon time reversal, which inverts electric currents and spins, but also upon spatial inversion, so that the *ferrotoroidic* state with a periodic arrangement of uniformly oriented toroidal moments (see figure 1(c)) can fill the remaining box in figure 2. According to (1) the free energy of the ferrotoroidic state is given by $F_{\text{fto}} = -\mathbf{T} \cdot \mathbf{G}$. Here, \mathbf{T} is the *toroidization* defined as toroidal moment per unit volume and named in analogy to the magnetization, polarization and deformation characterizing the other primary ferroic states. Since \mathbf{T} is odd under space-and time-inversion, the same holds for the field \mathbf{G} coupled to the toroidization, because the free energy must remain invariant upon these transformations.

2.2. Microscopic definition

The ferrotoroidic state was introduced in the previous section solely on the basis of the symmetry properties of its corresponding order parameter. We now elucidate its microscopic origin and discuss how to calculate the toroidization of magnetically ordered crystals. First we provide the formal definition of the toroidal moment, which appears

in the same order of the magnetic multipole expansion as the magnetic quadrupole moment.

2.2.1. Multipole expansion. Following Landau and Lifshitz [9], we consider a stationary distribution of classical electric currents $\mathbf{j}(\mathbf{x}) = \sum_{\alpha} e_{\alpha} \dot{\mathbf{r}}_{\alpha} \delta(\mathbf{x} - \mathbf{r}_{\alpha})$ and calculate the time-averaged magnetic field $\langle \mathbf{H}(\mathbf{R}) \rangle$ at some distant point \mathbf{R} . (In quantum mechanics the time average, here expressed by angle brackets, is replaced by the ground state expectation value or the thermal ensemble average.) The time-averaged electrodynamic vector potential $\langle \mathbf{A} \rangle$ satisfying $\langle \mathbf{H} \rangle = \nabla \times \langle \mathbf{A} \rangle$ and $\nabla \cdot \langle \mathbf{A} \rangle = 0$ is given by [9]

$$\langle \mathbf{A}(\mathbf{R}) \rangle = \frac{1}{c} \int d^3x \frac{\langle \mathbf{j}(\mathbf{x}) \rangle}{|\mathbf{R} - \mathbf{x}|} = \frac{1}{c} \left\langle \sum_{\alpha} \frac{e_{\alpha} \cdot \dot{\mathbf{r}}_{\alpha}}{|\mathbf{R} - \mathbf{r}_{\alpha}|} \right\rangle \quad (2)$$

and its multipole expansion has the form

$$\langle \mathbf{A}(\mathbf{R}) \rangle = \frac{1}{c} \sum_{n=0}^{\infty} \frac{(-)^n}{n!} \left\langle \sum_{\alpha} e_{\alpha} \dot{\mathbf{r}}_{\alpha} (r_{\alpha} \cdot \nabla)^n \frac{1}{R} \right\rangle. \quad (3)$$

For the zeroth-order term we obtain

$$\langle \mathbf{A} \rangle^{(0)} = c^{-1} \left\langle \sum_{\alpha} e_{\alpha} \dot{\mathbf{r}}_{\alpha} \right\rangle = 0 \quad (4)$$

since the average of a time derivative is zero, while for the first-order term we obtain

$$\langle \mathbf{A} \rangle^{(1)} = -\mathbf{m} \times \nabla \left(\frac{1}{R} \right), \quad (5)$$

where

$$\mathbf{m} = \frac{1}{2c} \left\langle \sum_{\alpha} e_{\alpha} \mathbf{r}_{\alpha} \times \dot{\mathbf{r}}_{\alpha} \right\rangle \quad (6)$$

is the magnetic dipole moment of the system.

The second-order term of the multipole expansion is the sum of the contributions from the magnetic quadrupole and toroidal moments. The quadrupolar part is

$$\langle \mathbf{A} \rangle_{\text{quadrupole}}^{(2)} = -\varepsilon_{ijk} q_{kl} \partial_j \partial_l \frac{1}{R}, \quad (7)$$

where

$$q_{ij} = \frac{1}{6c} \left\langle \sum_{\alpha} e_{\alpha} ([\mathbf{r}_{\alpha} \times \dot{\mathbf{r}}_{\alpha}]_i r_{\alpha j} + [\mathbf{r}_{\alpha} \times \dot{\mathbf{r}}_{\alpha}]_j r_{\alpha i}) \right\rangle \quad (8)$$

is the magnetic quadrupole moment. The toroidal part is

$$\langle \mathbf{A} \rangle_{\text{toroidal}}^{(2)} = \nabla (\mathbf{t} \cdot \nabla) \frac{1}{R} + 4\pi \mathbf{t} \delta(\mathbf{R}), \quad (9)$$

where

$$\mathbf{t} = \frac{1}{6c} \left\langle \sum_{\alpha} e_{\alpha} [\mathbf{r}_{\alpha} \times [\mathbf{r}_{\alpha} \times \dot{\mathbf{r}}_{\alpha}]] \right\rangle \quad (10)$$

$$= -\frac{1}{4c} \left\langle \sum_{\alpha} e_{\alpha} r_{\alpha}^2 \dot{\mathbf{r}}_{\alpha} \right\rangle \quad (11)$$

$$= -\frac{1}{4c} \left\langle \int d^3r r^2 \mathbf{j}(\mathbf{r}) \right\rangle \quad (12)$$

is the toroidal moment⁴. An alternative definition of the toroidal moment

$$\mathbf{t} = \frac{1}{10c} \left\langle \sum_{\alpha} (\mathbf{r}_{\alpha} (\mathbf{r}_{\alpha} \cdot \mathbf{j}_{\alpha}) - 2r_{\alpha}^2 \mathbf{j}_{\alpha}) \right\rangle, \quad (13)$$

commonly found in the literature [3, 6], is equivalent to (10) (see footnote 4).

The first term in (9) is the gradient of a scalar yielding zero magnetic field. The second term is zero away from the currents inducing the toroidal moment. Thus, the magnetic field generated by the toroidal moment is zero which may explain why it is usually not mentioned in textbooks on electromagnetism. However, the ‘contact term’ represented by the δ -function in (9) can play an important role (see appendix A). Note that the double outer product appearing in (10) for \mathbf{t} shows why electric currents circulating in the torus-shaped solenoid induce a toroidal moment (see figure 1(a)).

For systems in which magnetic fields are induced by spins, the current density, defined as the variational derivative of the energy with respect to the vector potential, is given by

$$\mathbf{j}_S = -c \frac{\delta}{\delta \mathbf{A}} \left\{ -g\mu_B \int d^3r \mathbf{s} \cdot [\nabla \times \mathbf{A}] \right\} \quad (14)$$

$$= cg\mu_B [\nabla \times \mathbf{s}], \quad (15)$$

where g is the gyromagnetic ratio, μ_B is the Bohr magneton and $\mathbf{s}(\mathbf{r})$ is the spin density.

Equation (13) with $\mathbf{j} = \mathbf{j}_S$ then gives

$$\mathbf{t} = \frac{g\mu_B}{2} \left\langle \int d^3r \mathbf{r} \times \mathbf{s}(\mathbf{r}) \right\rangle. \quad (16)$$

In the limit where the spin density consists of localized spins \mathbf{S}_{α} each with magnetic moment $\mathbf{m}_{\alpha} = g\mu_B \mathbf{S}_{\alpha}$, i.e.

$$\mathbf{s}(\mathbf{r}) = \sum_{\alpha} \mathbf{S}_{\alpha} \delta(\mathbf{r} - \mathbf{r}_{\alpha}), \quad (17)$$

we obtain the expression for the toroidal moment for a configuration of localized spins:

$$\mathbf{t} = \frac{g\mu_B}{2} \left\langle \sum_{\alpha} [\mathbf{r}_{\alpha} \times \mathbf{S}_{\alpha}] \right\rangle \quad (18)$$

$$= \frac{1}{2} \left\langle \sum_{\alpha} [\mathbf{r}_{\alpha} \times \mathbf{m}_{\alpha}] \right\rangle. \quad (19)$$

In this case the toroidal moment is ‘the moment of magnetization’.

In the following sections we discuss two difficulties associated with the direct application of (19) to the calculation of the toroidal moment: the dependence on the choice of origin and the application to bulk, periodic solids. Henceforth, the averaging brackets are omitted for brevity.

⁴ For the double outer product we find $\mathbf{r} \times [\mathbf{r} \times \dot{\mathbf{r}}] = \mathbf{r}(\mathbf{r} \cdot \dot{\mathbf{r}} - r^2 \dot{r})$. The first term in this expression can be rewritten as $\mathbf{r}(\mathbf{r} \cdot \dot{\mathbf{r}}) = \frac{1}{2} \mathbf{r} \frac{d}{dt} r^2 = \frac{1}{2} \frac{d}{dt} (r\mathbf{r}^2) - \frac{1}{2} r^2 \dot{\mathbf{r}}$. As mentioned above, the average of a time derivative is zero so that $\langle \frac{d}{dt} (r\mathbf{r}^2) \rangle = 0$, so that $\langle \mathbf{r} \times [\mathbf{r} \times \dot{\mathbf{r}}] \rangle = -\langle \frac{3}{2} r^2 \dot{\mathbf{r}} \rangle$, which explains the equivalence of (10) and (11). The equivalence of (10) and (13) can be proved in a similar way.

2.2.2. *Coupling to magnetic field and origin dependence of toroidal moment.* For systems with a net magnetization, \mathbf{M} , the toroidal moment obtained from (13), (16) or (19) clearly depends on the choice of origin used in determining the position, \mathbf{r} . This is a result of the fact that, for systems with nonzero magnetization, the higher-order multipoles are not in fact extensive quantities. We can see this by considering a spin system in an inhomogeneous magnetic field $\mathbf{H}(\mathbf{r})$ that varies slowly on the scale of the system size. Then the interaction energy, H_{int} , of spins with the magnetic field

$$H_{\text{int}} = -g\mu_B \sum_{\alpha} \mathbf{S}_{\alpha} \cdot \mathbf{H}(\mathbf{r}_{\alpha}) \quad (20)$$

can be expanded in powers of field gradients calculated at some arbitrary reference point $\mathbf{r} = 0$:

$$H_{\text{int}} = -g\mu_B \sum_{\alpha} \mathbf{S}_{\alpha} \cdot \mathbf{H}(0) - g\mu_B \sum_{\alpha} r_{\alpha i} S_{\alpha j} \partial_i H_j(0) - \dots \quad (21)$$

The first term is the interaction of the field with the magnetic moment of the system

$$\mathbf{m} = g\mu_B \sum_{\alpha} \mathbf{S}_{\alpha}. \quad (22)$$

In the second term, the tensor $\mathcal{M}_{ij} = g\mu_B \sum_{\alpha} r_{\alpha i} S_{\alpha j}$ with nine components can be decomposed into three parts: (i) the pseudoscalar

$$a = \frac{1}{3} \mathcal{M}_{ii} = \frac{g}{3} \mu_B \sum_{\alpha} \mathbf{r}_{\alpha} \cdot \mathbf{S}_{\alpha}, \quad (23)$$

(ii) the toroidal moment vector

$$\mathbf{t} = \frac{g}{2} \mu_B \sum_{\alpha} \mathbf{r}_{\alpha} \times \mathbf{S}_{\alpha}, \quad (24)$$

dual to the antisymmetric part of the tensor, $t_i = \frac{1}{2} \epsilon_{ijk} \mathcal{M}_{jk}$, (iii) the traceless symmetric tensor q_{ij} describing the quadrupole magnetic moment of the system,

$$q_{ij} = \frac{1}{2} (\mathcal{M}_{ij} + \mathcal{M}_{ji} - \frac{2}{3} \delta_{ij} \mathcal{M}_{kk}) \quad (25)$$

$$= \frac{g}{2} \mu_B \sum_{\alpha} \left[r_{\alpha i} S_{\alpha j} + r_{\alpha j} S_{\alpha i} - \frac{2}{3} \delta_{ij} \mathbf{r}_{\alpha} \cdot \mathbf{S}_{\alpha} \right]. \quad (26)$$

The terms up to first order in the expansion of (21) can then be written in the form

$$H_{\text{int}} = -\mathbf{m} \cdot \mathbf{H}(0) - a (\nabla \cdot \mathbf{H})_{\mathbf{r}=0} - \mathbf{t} \cdot [\nabla \times \mathbf{H}]_{\mathbf{r}=0} - q_{ij} (\partial_i H_j + \partial_j H_i)_{\mathbf{r}=0}. \quad (27)$$

The pseudoscalar a is coupled to the divergence of magnetic field, which in the absence of magnetic monopoles is zero, while the toroidal moment \mathbf{t} couples to the curl of the magnetic field, which is only nonzero in presence of electric current flowing through the system.

If the magnetic moment \mathbf{m} of the system is nonzero, the first term in the expansion (27) depends on the point at which the magnetic field and its gradient are calculated. Since the total magnetic interaction energy is independent of the choice of origin, this gives rise to a corresponding dependence in the moments a , \mathbf{t} and q_{ij} . For example, the toroidal moments, \mathbf{t}_R

and t_0 , appearing in the expansion around, respectively, $r = R$ and $r = 0$, are related by

$$t_R = t_0 - \frac{1}{2}R \times m. \quad (28)$$

More generally, if the magnetic moment of a system is nonzero, the higher multipole moments are not necessarily extensive and shape-independent quantities. One obvious example is the toroidal moment of a spin vortex with $m(r) = m_0 e_\varphi$ in a disc of radius R ; this grows as R^3 , whereas the volume of the disc increases only as R^2 . On the other hand, for zero magnetization, the extensive parts of a , t and q_{ij} are intrinsic properties of the system and describe the symmetry breaking in the magnetically ordered state.

One practical way to proceed in the discussion of toroidal moments in systems with nonzero net magnetization is to separate the general magnetization distribution into a ‘compensated’ part, which has no net magnetization, and a uniform background ‘uncompensated’ part, which corresponds to the average magnetization of the system. The latter does not break space-inversion symmetry and therefore does not contribute to the toroidization of the system. Such a decomposition was achieved effectively in earlier work by choosing the ‘centre of the unit cell’ as the origin, so that magnetizations of equal magnitude were placed at equal positive and negative distances from the origin [10, 11]. We will also show in the following that *change* in toroidization for example during a structural distortion is usually the quantity of interest. Since a structural distortion leaves the apparent toroidization resulting from the uniform background magnetization unchanged, the change in toroidization is not origin dependent provided that a consistent choice of origin is made [5].

2.2.3. Calculation for a periodic system. The quantitative evaluation of the toroidal moment of a given magnetization density can in principle be achieved using (16) or (19) if the magnetization consists of localized point magnetic moments provided that the system is finite. Evaluation of the macroscopic toroidization for a bulk periodic system can not, however, be performed by direct application of either (16) or (19). In fact, the problems encountered are similar to those faced in the evaluation of electric polarization in bulk periodic solids. Here we review the now-well-established concepts of the polarization lattice and polarization quantum in bulk periodic solids [12]. This provides a basis for the formalism that was recently introduced in [5] for the definition of toroidization in bulk periodic solids.

Polarization in bulk periodic solids. The difficulties associated with the calculation of polarization in bulk periodic solids are illustrated in figure 3(a) for the simplest case of a one-dimensional chain of localized ionic charges. Here the polarization, defined as the dipole moment per unit volume (or per unit length in this one-dimensional case), has an apparent unphysical dependence on the choice of the unit cell selected to evaluate it. For the left-hand unit cell, the dipole moment per

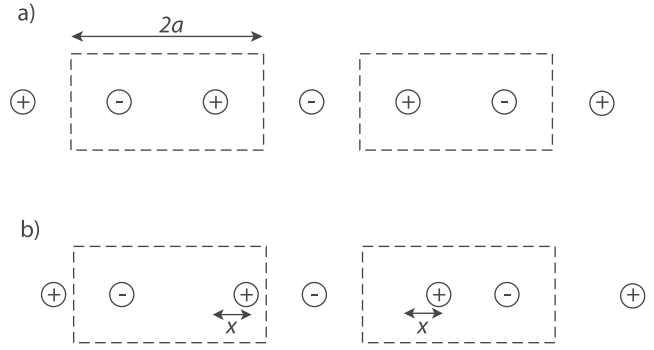


Figure 3. Calculation of the polarization in a bulk periodic solid. (a) illustrates the dependence of the absolute value of the polarization on the choice of unit cell; the two choices shown here differ by one polarization quantum. (b) shows that *changes* in polarization are well defined, independently of the choice of unit cell or basis.

unit length is

$$P = \frac{1}{2a} \sum_i q_i r_i \quad (29)$$

$$= \frac{1}{2a} \left(+\frac{a}{2} - \frac{3a}{2} \right) e \quad (30)$$

$$= -\frac{1}{2}e, \quad (31)$$

whereas for the right-hand unit cell,

$$P = \frac{1}{2a} \left(-\frac{a}{2} + \frac{3a}{2} \right) e \quad (32)$$

$$= +\frac{1}{2}e. \quad (33)$$

Other choices of unit cell and/or basis yield polarizations that differ from each other by integer multiples of the so-called ‘polarization quantum’ are possible, which correspond to the change in polarization on moving one electronic charge e a distance of one unit cell. The polarization of a bulk periodic solid, therefore, is not given by a single number, but is rather a *lattice* of values separated from each other by polarization quanta.

Changes in polarization, however, are uniquely defined quantities, as illustrated in figure 3(b), where the cations have been shifted a distance x to the right relative to their positions in (a). For both the left and right unit cells, the change in polarization,

$$\delta P = \frac{1}{2a} \sum_i q_i \delta r_i \quad (34)$$

$$= \frac{1}{2a} (+x - 0) e \quad (35)$$

$$= \frac{x e}{2a}. \quad (36)$$

Since experimentally only changes in polarization can be determined there is in fact no inconsistency between the theoretical and experimental formalisms.

2.2.4. Toroidization in bulk periodic solids. As pointed out above, in a bulk periodic solid, translation of an

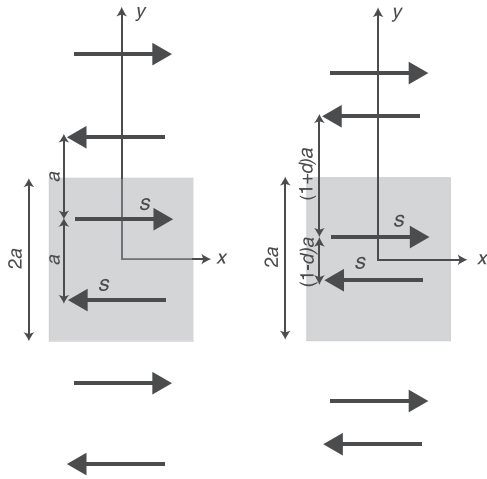


Figure 4. Calculation of the change in toroidization from a non-toroidal reference structure (left) to a structure with a net toroidization (right). The difference in toroidization values between the two structures should be interpreted as the spontaneous toroidization.

electronic charge by a lattice vector \mathbf{R} does not change the overall arrangement, but does change the polarization by the polarization quantum, $e\mathbf{R}/\Omega$, where Ω is the volume of the primitive unit cell. Likewise, translation of a *spin*, \mathbf{S} by a lattice vector leaves the system unchanged, but changes the *toroidization* by

$$\Delta \mathbf{T} = \frac{g\mu_B}{2\Omega} \mathbf{R} \times \mathbf{S}. \quad (37)$$

Therefore the toroidization in a bulk periodic solid is not single-valued. By analogy with the polarization case, we call the resulting multiple values of the toroidization a *toroidization lattice*, and for the quantity $\Delta \mathbf{T}$ we propose the term *toroidization increment* [5].

This apparently unphysical situation is resolved again, however, by the fact that *changes* in toroidization are uniquely defined. Therefore, in principle, the change in toroidization relative to a non-toroidal reference structure which preserves space-inversion and time reversal symmetry can always be calculated; this is the physically meaningful quantity.

In figure 4 we illustrate the calculation of the change in toroidization from a non-toroidal reference structure (left panel); for a more detailed discussion see [5]. The multiple allowed values of the toroidization for the non-toroidal reference structure are $\mathbf{T}_n = (\frac{1}{2} + n)\frac{1}{2}\hat{z}$, where n is any integer. When the magnetic ions shift a distance d from their centrosymmetric positions to form antiferromagnetic dimers (right panel), the allowed values for the toroidization are

$$\mathbf{T}_n(d) = \left(n - \frac{1-d}{2} \right) \frac{s}{2} \hat{z}. \quad (38)$$

The change in toroidization between the two configurations is identical for any branch n . For example, for the shaded unit cell, the toroidization of the non-toroidal structure is $-\hat{z}/4$ and that of the left panel is $-(1-d)s\hat{z}/4$, so the change in toroidization is $sd\hat{z}/4$. By analogy to the electrical polarization this can be interpreted as the *spontaneous toroidization* of the toroidal structure [5].

2.3. Relation between toroidal moment and $\mathbf{P} \times \mathbf{M}$

As discussed above, the toroidal moment is a vector changing sign under both time reversal and space-inversion symmetry. However, not every vector changing sign under time reversal and space-inversion symmetry is a toroidal moment. A number of recent papers have labelled the cross product $\mathbf{P} \times \mathbf{M}$ —which has the same symmetry as \mathbf{T} —as a ‘toroidal moment’ [13–15]. While $\mathbf{P} \times \mathbf{M}$ indeed seems to be a useful quantity for describing the behaviour of multiply ferroic systems with coupled macroscopic polarization and magnetization [18], we emphasize that it is not in fact a toroidal moment as defined formally by (13). Here ‘multiply ferroic’ refers to composites with a ferromagnetic and a ferroelectric constituent displaying the magnetoelectric effect as product effect [4], or multilayer heterostructures with strong correlations across the interface [15–17]. The coupling $[\mathbf{P} \times \mathbf{M}] \cdot [\mathbf{E} \times \mathbf{H}]$, which is allowed by symmetry in these systems, leads to a magnetoelectric response similar to that of ferrotoroidics, such as a tilt of electric polarization of a conical spiral in response to an applied magnetic field [18]. However, $\mathbf{P} \times \mathbf{M}$ is not necessarily coupled to $\nabla \times \mathbf{H}$ as in (27), which is required for a toroidal moment.

3. Macroscopic definition and relationship to the magnetoelectric effect

The most direct evidence for the presence of ferrotoroidic order would be the observation of its macroscopic toroidization in analogy to, e.g., ferromagnetism which is detected via its macroscopic magnetization. However, because a probe directly measuring a toroidization still needs to be developed (see section 6.1) present attempts at observing ferrotoroidic order are aimed at measuring responses which couple to the ferrotoroidic order parameter. Using the coupling $-\mathbf{T} \cdot \nabla \times \mathbf{H}$ is problematic because the curl of the magnetic field corresponds to an electric current that has to flow through a magnetic insulator, and furthermore, variations of external magnetic fields on the scale of one unit cell are very small.

We will now show that indirect evidence for the presence of a spontaneous toroidal moment in a system can be obtained by measuring the linear magnetoelectric effect, which is introduced via an expansion of the free energy [19], i.e.,

$$\tilde{F}(\mathbf{E}, \mathbf{H}) = F_0 - \frac{\varepsilon_{ij} E_i E_j}{8\pi} - \frac{\mu_{ij} H_i H_j}{8\pi} - \alpha_{ij} E_i H_j + \dots \quad (39)$$

where ε_{ij} , μ_{ij} and α_{ij} are, respectively, the dielectric permittivity, the magnetic permeability and the so-called *magnetoelectric tensor*. Using $\partial \tilde{F} / \partial \mathbf{E} = -\mathbf{D}/4\pi$ and $\partial \tilde{F} / \partial \mathbf{H} = -\mathbf{B}/4\pi$, we obtain

$$P_i = \chi_{ij}^e E_j + \alpha_{ij} H_j, \quad (40)$$

$$M_i = \alpha_{ji} E_j + \chi_{ij}^m H_j,$$

where $\chi_{ij}^e = (\varepsilon_{ij} - \delta_{ij})/4\pi$ and $\chi_{ij}^m = (\mu_{ij} - \delta_{ij})/4\pi$ are, respectively, the dielectric and magnetic susceptibility tensors. When the magnetoelectric tensor is nonzero, an applied electric field induces a magnetization and an applied magnetic field induces an electric polarization.

It follows from (39) that the magnetoelectric tensor α_{ij} changes sign upon $\mathbf{r} \rightarrow -\mathbf{r}$ or $t \rightarrow -t$, so that a linear magnetoelectric effect requires a simultaneous violation of spatial inversion symmetry and time reversal symmetry. Therefore, it can occur in magnetically ordered systems where spin ordering breaks the spatial inversion symmetry. These are precisely the conditions allowing the magnetic multipoles a , \mathbf{t} and q_{ij} , discussed in section 2.2.2, to be nonzero. In turn, these magnetic multipole orders can give rise to a linear magnetoelectric effect.

The 3×3 matrix α_{ij} can also be decomposed into a pseudoscalar, a vector and a symmetric traceless tensor,

$$\tilde{F}_{\text{me}} = -\tilde{a} (\mathbf{E} \cdot \mathbf{H}) - \tilde{\mathbf{t}} \cdot [\mathbf{E} \times \mathbf{H}] - \tilde{q}_{ij} (E_i H_j + E_j H_i), \quad (41)$$

in complete analogy with the multipole decomposition of the tensor \mathcal{M}_{ij} into the a , \mathbf{t} and q_{ij} in (27). By symmetry a nonzero \mathcal{M}_{ij} implies that the corresponding component of α_{ij} is also nonzero. Thus, in the state with the toroidal moment $\mathbf{t} \neq 0$, an electric polarization is induced along the applied magnetic field and vice versa, according to

$$\begin{aligned} \mathbf{P} &= -\tilde{\mathbf{t}} \times \mathbf{H}, \\ \mathbf{M} &= \tilde{\mathbf{t}} \times \mathbf{E}. \end{aligned} \quad (42)$$

It is difficult (if not impossible) to give a general relation between magnetic multipoles and the corresponding components of the magnetoelectric tensor. Physically, the magnetoelectric effect involves shifts of ions and polarization of electronic orbitals induced by changes in orientations of spins, while magnetic multipoles merely describe the spin configuration of the system. Mathematically, the magnetoelectric tensor is obtained by calculating the *second-order correction* to the free energy in external electric and magnetic fields, while magnetic multipoles are generated by the expansion of the *first-order correction* to the free energy in powers of the gradients of magnetic field (see (27)).

Furthermore, magnetic multipole ordering is not the only source of the magnetoelectric effect, and while a toroidal moment always gives rise to an off-diagonal magnetoelectric response, such a response is not necessarily indicative of a toroidal moment. For example, conical spiral ordering, described by

$$\mathbf{M}_n = M_{\parallel} \hat{z} + M_{\perp} (\hat{x} \cos Qz_n + \hat{y} \sin Qz_n) \quad (43)$$

with the spin rotation axis \hat{z} parallel to the propagation vector Q of the spiral, gives rise to a linear magnetoelectric effect with nonzero antisymmetric contributions $\alpha_{xy} = -\alpha_{yx}$: a magnetic field applied along \hat{x} will cant the cone axis (but not Q) in the same direction resulting in a cycloidal yz -spiral component, which induces an electric polarization along the y axis [20, 21]. Similarly, a magnetic field applied along the y axis will induce a polarization in the x direction. Such a magnetoelectric behaviour $\tilde{\mathbf{t}} \parallel z$ in conical spiral state was observed in the ZnCr_2Se_4 spinel [22, 23]. Nevertheless the toroidal moment \mathbf{t} of this state calculated using (24), is zero!

4. Upper bound on magnetoelectric susceptibility and its microscopic origin

4.1. Thermodynamic inequalities

Thermodynamic stability requires the components of the inverse dielectric permittivity tensor and the inverse magnetic permeability tensor to be positive [19]:

$$(\varepsilon^{-1})_{ij} = \frac{\partial E_i}{\partial D_j} > 0, \quad (\mu^{-1})_{ij} = \frac{\partial H_i}{\partial B_j} > 0. \quad (44)$$

(Here, all partial derivatives are calculated at constant temperature and chemical potential.)

These considerations can be extended to obtain an upper bound on the components of the magnetoelectric tensor [24]. Thermodynamic stability requires that the free energy $F(\mathbf{D}, \mathbf{B}) = \tilde{F}(\mathbf{E}, \mathbf{H}) + \mathbf{E} \cdot \mathbf{D}/4\pi + \mathbf{H} \cdot \mathbf{B}/4\pi$ has an absolute minimum at $\mathbf{D} = \mathbf{B} = 0$, or equivalently, the free energy $\tilde{F}(\mathbf{E}, \mathbf{H})$ must have an absolute maximum at zero electric and magnetic fields. For this the 6×6 matrix

$$\begin{pmatrix} \varepsilon & 4\pi\alpha \\ 4\pi\alpha^T & \mu \end{pmatrix}, \quad (45)$$

has to be positive definite (here $\alpha_{ij}^T = \alpha_{ji}$), from which one obtains the upper bound on the component of magnetoelectric tensor,

$$|\alpha_{ij}| \leq \frac{\sqrt{\varepsilon_{ii}\mu_{jj}}}{4\pi}. \quad (46)$$

In [25] a general expression for the magnetoelectric tensor is obtained within the second-order thermodynamic perturbation theory. Neglecting diamagnetic susceptibility, which for magnetic materials is small compared to their paramagnetic susceptibility, they found the stronger condition

$$\alpha_{ij} \leq \sqrt{\chi_{ii}^e \chi_{jj}^m}, \quad (47)$$

which limits the components of the magnetoelectric tensor by the geometric mean of the corresponding dielectric and magnetic susceptibilities.

Equation (47) provides a rather stringent upper bound on α_{ij} : most commonly, the linear magnetoelectric effect is found in collinear antiferromagnets with a magnetic susceptibility $\chi^m \ll 1$. The upper limit on the magnetoelectric susceptibility can be higher in frustrated spin systems, where the competition between nearly degenerate spin states often gives rise to relatively large magnetic susceptibilities and phase transitions induced by applied fields [26]. In addition, studying the magnetoelectric properties of frustrated systems is promising because frustration often results in spin arrangements breaking inversion symmetry—a necessary condition for the magnetoelectric effect. Frustrated systems are therefore a potential source of giant magnetoelectric response with magnetic-field-induced electric phase transitions or vice versa.

Another way to increase the upper bound on the coupling constant α_{ij} is to look for magnetoelectric materials showing ferroelectric and/or ferromagnetic transitions and, hence, a

large electric permittivity and/or magnetic permeability. We note that the conditions in (46) and (47) also hold for materials with a spontaneous electric polarization $P_{\text{sp}} \neq 0$ and/or spontaneous magnetization $M_{\text{sp}} \neq 0$, provided that they are in a uniform stable or metastable state. Such systems, however, can easily be driven away from equilibrium and their magnetic/dielectric response is often dominated by the domain wall motion, in which case the upper bounds (46) and (47) do not apply. This non-equilibrium dynamics can lead to large observable magnetoelectric effects.

Such a divergence of magnetoelectric susceptibility is found in boracites, $M_3B_7O_{13}X$, where M is a divalent metal ion and X is a halogen. These materials become ferroelectric at an elevated temperature ($T_{\text{FE}} = 466$ K for the Co–Br boracite), while at a temperature $T_c = 10\text{--}40$ K some of them show a transition into a magnetoelectric state which is weakly ferromagnetic [27]. Below T_c the components α_{23} and α_{32} have a very different temperature dependence. In particular, α_{32} shows a sharp peak at T_c , while α_{23} does not.

As was shown by Sannikov, these observations can be explained if one assumes that below T_c the boracites become ferrotoroidically ordered [28, 29]. First, free-energy contributions of the type

$$\Phi_{\text{me}} = -\lambda T_1 (P_3 M_2 - P_2 M_3) \quad (48)$$

where T , M and P are, respectively, spontaneous toroidization, magnetization and polarization, gives rise to an antisymmetric magnetoelectric effect coupling linearly to the toroidal order parameter: $\alpha_{32} - \alpha_{23} \propto T_1$. Second, if the toroidal ordering occurs in the ferroelectric state with $P_3 \neq 0$, as it does in the boracites, it automatically induces a magnetization $M_2 \propto P_3 T_1$. Furthermore, since the magnetization M_2 is linearly coupled to the primary order parameter T_1 , the vanishing rigidity with respect to fluctuations of the toroidal moment at T_c results in the divergence of the magnetic susceptibility χ_{22}^m below the critical temperature:

$$\chi_{22}^m \propto \frac{1}{T_c - T}. \quad (49)$$

As the dielectric susceptibility χ_{33}^e stays finite at T_c , the divergent part of the magnetoelectric tensor α_{32} cannot grow faster than

$$\alpha_{32} \propto \frac{1}{\sqrt{T_c - T}}, \quad (50)$$

but it is still divergent in agreement with the experimental observation [28, 29].

4.2. Microscopic mechanisms for magnetoelectric coupling

Microscopic mechanisms for linear magnetoelectric coupling, briefly discussed in [30], are similar to those coupling polarization and magnetism in the spiral multiferroic materials [31–33]. One mechanism—the spin-lattice coupling—results from the dependence of exchange interactions (such as isotropic Heisenberg exchange or anisotropic Dzyaloshinskii–Moriya interaction) on the relative positions of magnetic and ligand ions. Consider an oxygen anion connecting two magnetic cations as shown in figure 5. The superexchange constant

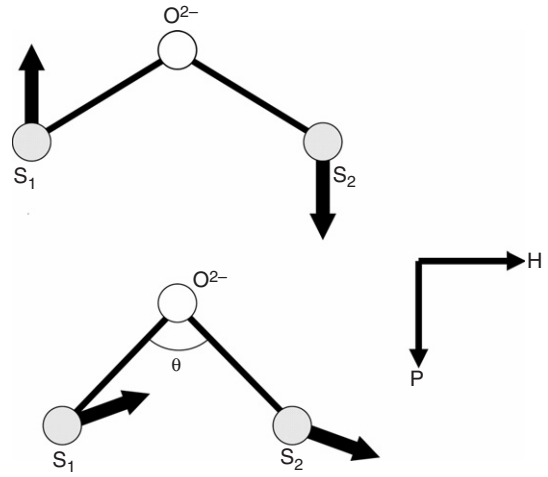


Figure 5. The spins of two transition metal ions (shaded circles) interacting via superexchange through an oxygen ion (empty circle). The upper figure shows the positions of the ions at zero magnetic field. As shown in the lower figure, the decrease of the angle between the spins in an applied magnetic field pushes the negatively charged oxygen ion away from the positively charged transition metal ions which induces an electric dipole moment.

sensitively depends on the metal–oxygen–metal bond angle θ ; according to the Anderson–Kanamori–Goodenough rules [34] the exchange is antiferromagnetic for $\theta = 180^\circ$ and ferromagnetic for $\theta = 90^\circ$. In an applied magnetic field the angle between spins therefore decreases, resulting in a decrease of the bond angle θ . The shift of the negative oxygen ion with respect to the positively charged transition metal ions induces an electric dipole moment.

Magnetoelectric effects can also originate in purely electronic mechanisms such as spin-dependent virtual electronic excitation of states within the scope of the superexchange process. For example, the state in which one electron is virtually transferred from magnetic site 1 to magnetic site 2 in figure 6, possesses an electric dipole moment oriented along the 1–2 direction. It is, however, exactly compensated by the dipole moment of the state in which an electron from site 2 is virtually transferred to site 1. On the other hand, the state with two holes on the oxygen ion and an extra electron on the sites 1 and 2 gives a nonzero contribution to the spin-dependent electric dipole in the direction orthogonal to the bond. Estimates show that the magnetoelectric coupling from electronic polarization is comparable to that from spin–lattice interaction [35].

5. Experimental observation of the ferrotoroidic state

In the preceding sections we introduced the concept of toroidal moments and ferrotoroidic order on the basis of macroscopic symmetry considerations as well as through a microscopic multipole expansion, and we investigated the relation between ferrotoroidicity and the magnetoelectric effect. In this section we address the question of whether ferrotoroidic order is actually observed in nature and how it can be observed and quantified. According to the Neumann principle, visualization of the ferrotoroidic state requires an experimental technique

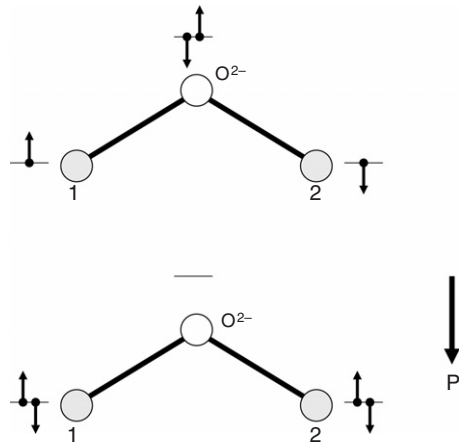


Figure 6. The upper figure shows an initial state of the superexchange process with a filled oxygen orbital. The lower shows the virtually excited state with two oxygen holes; this has a dipole moment due to the redistribution of the electrons. This virtual excitation is only possible if spins on neighbouring transition metal sites are initially antiparallel.

that is based on an effective coupling to the violation of spatial as well as temporal inversion symmetry as an inherent property of the ferrotoroidic order parameter. Several approaches have been realized thus far and will be discussed in the following.

5.1. Magnetoelectric effect

As discussed in section 3 antisymmetric contributions $\alpha_{ij} = -\alpha_{ji}$ to the magnetoelectric effect can couple to the ferrotoroidic order parameter. In general, the magnetoelectric effect is composed of symmetric as well as antisymmetric contributions so that observation of a component $\alpha_{ij} \neq \alpha_{ji}$ is already an indication for the presence of ferrotoroidic order. This was first achieved in $\text{Co}_3\text{B}_7\text{O}_{13}\text{Br}$ and related boracite compounds where α_{23} and α_{32} were measured [36] as discussed in section 4.1. Subsequently, asymmetries of magnetoelectric contributions were reported for $\text{Ga}_{2-x}\text{Fe}_x\text{O}_3$ [37] and Cr_2O_3 [38]. In Cr_2O_3 the ferrotoroidic state is only present when above a critical magnetic field $H_c \parallel z$ the magnetic Cr^{3+} moments are flopped from the z axis into the xy plane. Consequently, the splitting between α_{13} and α_{31} is present above H_c only.

Although measurement of the magnetoelectric effect is a very convenient way for detecting ferrotoroidicity it must not be forgotten that this is an indirect approach. In particular it was shown in section 3 that the observation of tensor components $\alpha_{ij} = -\alpha_{ji}$ does *not uniquely* indicate the presence of ferrotoroidic order. In this respect, the most convincing evidence for ferrotoroidicity thus far was found in boracite compounds like $\text{Co}_3\text{B}_7\text{O}_{13}\text{Br}$. In [29] and as summarized in section 4.1 it was shown that in the boracite compounds an expansion of the free energy in polarization, magnetization and toroidization with the latter taken as order parameter leads to a divergence of α_{32} near the temperature of the transition to the $m'm2'$ phase allowing ferrotoroidic order. Observation of this divergence constituted a direct

confirmation of the concept of ferrotoroidicity because it directly evidenced the existence of an order parameter as a characteristic feature of the ferroic state. In addition, it provides an explicit expression for the relation between ferrotoroidicity and the antisymmetric magnetoelectric effect for this specific case.

5.2. X-ray gyrotropy and dichroism

The first examples of x-ray diffraction coupling to space-inversion and time reversal symmetry breaking were reported for antiferromagnetic compounds in which the spin arrangement of the time reversal symmetry breaking magnetic order also breaks spatial inversion symmetry. These effects were investigated with circularly polarized x-rays on V_2O_3 and Cr_2O_3 . The terms nonreciprocal x-ray gyrotropy [39] and magnetochiral x-ray dichroism [40, 41] are used, depending on whether a reversal of the real or the imaginary part of a component of the gyration tensor is observed upon reversal of the magnetic order parameter. However, an investigation of ferrotoroidic materials has not yet occurred. It was claimed that the magnetochiral dichroism couples to the orbital anapole moment, i.e., the orbital contribution to the toroidal moment (see appendix A) but this claim contradicts the non-ferrotoroidic symmetry of Cr_2O_3 in zero field and further verifications have not yet been made.

Subsequently, x-ray directional (i.e., magnetochiral) dichroism was investigated on a polar ferromagnet, GaFeO_3 . A change of absorption upon magnetization reversal was demonstrated and interpreted as being equivalent to a sign reversal of $\mathbf{P} \times \mathbf{M}$. However, as discussed in section 2.3 this term does not necessarily couple to a toroidal moment. Furthermore, the change of absorption upon polarization reversal also needs to be demonstrated in order for an interpretation in terms of $\mathbf{P} \times \mathbf{M}$ (instead of \mathbf{M}) to be meaningful.

5.3. Linear optical effects

In the visible range a dichroic linear optical effect changing sign under space and time reversal was demonstrated on luminescent tris(3-trifluoroacetyl-6-camphorato) europium(III) complexes. The intensity of the luminescence light emitted around 620 nm upon UV excitation was measured in dependence of the direction of a magnetic field for the two enantiomers of the compound [42]. Field reversal and a change of enantiomers led to the same change of luminescence intensity thus confirming the coupling to the space and time asymmetry in separate experiments. Although this is a very convincing result the luminescence technique is applicable to certain organic molecules but not to ferrotoroidic materials in general.

Sensitivity to the orientation of the space and time reversal symmetry breaking antiferromagnetic order of Cr_2O_3 was demonstrated in a linear reflection experiment. A reversal of the order parameter reversed the angle of rotation of the reflected light detected as a reflectivity change of the order of 10^{-5} , an effect called nonreciprocal reflection [43].

5.4. Nonlinear optical effects

If light fields described by the vector potentials $\mathbf{A}(\omega_1)$, $\mathbf{A}(\omega_2)$, etc are incident on a crystal they induce source terms $\mathbf{S}(\omega_{\text{NL}})$ of electromagnetic waves at frequencies $\omega_{\text{NL}} = \sum_{i=1}^N n_i \omega_i$ where N is the number of wave fields participating in the excitation and $n_i \in \mathbb{Z}$ [45, 46]. The simplest nonlinear optical process is electric dipole (ED) type second harmonic generation (SHG) which is described by

$$\mathbf{P}(2\omega) = \frac{c}{4\pi} \hat{\chi}^{(2)} \mathbf{E}(\omega) \mathbf{E}(\omega) \quad (51)$$

where the intensity of the SHG wave emitted from the crystal, $I_{\text{SHG}} \propto |\mathbf{S}|^2$, and $\mathbf{S} = (4\pi/c) \partial^2 \mathbf{P} / \partial t^2$. The susceptibility $\hat{\chi}$ describes the nonlinear optical response of the medium and is determined by its symmetry and microscopic structure. Following the Neumann principle, the symmetry determines the set of tensor components $\chi_{ijk} \neq 0$. Long-range ordering affects the symmetry. This leads to contributions $\propto \hat{\chi}(\hat{O})$ to the SHG, which couple, in first order, linearly to the order parameter \hat{O} so that $\hat{\chi}(-\hat{O}) = -\hat{\chi}(\hat{O})$. Thus, SHG light from opposite domains has a 180° phase shift which allows one to identify the domain structure [47]. Since each form of (anti)ferroic order affects symmetry in a different way the SHG contributions from $\hat{\chi}(\hat{O}_1)$, $\hat{\chi}(\hat{O}_2)$, etc in a multiferroic are in general differently polarized. This allows one to image even coexisting domain structures by polarization analysis [48].

For the first time SHG coupling to space and time parity violation was observed in Cr_2O_3 where a SHG contribution coupling linearly to the antiferromagnetic order parameter was detected and used for imaging the (non-ferrotoroidic) domain structure [49, 50]. Similar experiments were performed on ferroelectric antiferromagnetic YMnO_3 [51] and on weakly ferromagnetic CuB_2O_4 [52]. An important step followed when finally ferrotoroidic domains were imaged by SHG in LiCoPO_4 , and shown to coexist with independent antiferromagnetic domains. The emergence of the toroidization in LiCoPO_4 is shown in figure 7(a) while figure 7(b) displays the coexistence of ferrotoroidic and antiferromagnetic domains in the compound.

SHG coupling to a state with nonzero toroidization was also claimed for ferromagnetic ratchet superlattices with broken inversion symmetry [53]. However, in this case the actual coupling demonstrated was to the magnetization, and the relation to the toroidization remains ambiguous.

6. Interesting perspectives of ferrotoroidicity

So far we have seen that the concept of ferrotoroidic order is reasonable from the point of view of space–time symmetry considerations as well as from the point of view of the multipole expansion of the electrodynamic vector potential. Long-range ordering of toroidal moments displaying salient features of a ferroic state have been observed: the existence of a ferrotoroidic order parameter was derived from magnetoelectric measurements and the existence of ferrotoroidic domains was proved by optical second harmonic generation. In spite of these achievements important questions

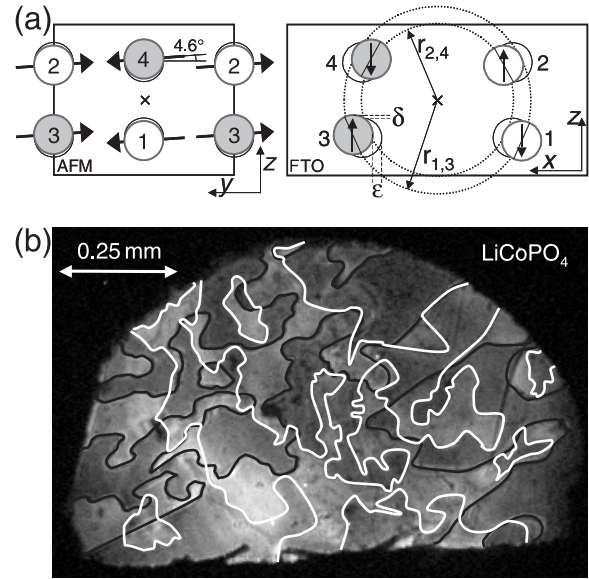


Figure 7. Observation of ferrotoroidic domains by optical SHG. (a) Distribution of Co^{2+} ions and their magnetic moments in the yz and xz planes. Co^{2+} ions at $x \sim \frac{3}{4}$ (filled) and $x \sim \frac{1}{4}$ (open) and shifts δ and ϵ from the high-symmetry position marked by thin black circles are shown. For clarity, spin components in the xz plane are magnified by 5 and the weak magnetization along the y axis is omitted. The dotted circles graphically visualize the origin of the toroidal moment. Because of $\mathbf{T} \propto \sum_n \mathbf{r}_n \times \mathbf{S}_n$ only the projections of S_z onto these circles contribute to T_y (see also [44]). Due to $r_{1,3} > r_{2,4}$ the clockwise and counterclockwise contributions do not cancel. A change of sign of S_x or φ corresponds to a reversal of the antiferromagnetic or ferrotoroidic order parameter, respectively. (b) Coexisting antiferromagnetic and ferrotoroidic domains of a LiCoPO_4 (100) sample at 10 K imaged with SHG light at 2.197 eV. Bright and dark areas are caused by the interference of antiferromagnetic and ferrotoroidic contributions to SHG. Black and white lines indicate the antiferromagnetic and the ferrotoroidic domain walls, respectively.

related to the ferroic nature of the ferrotoroidic state remain unanswered. Controlled switching of ferrotoroidic domains by a toroidal field has not been accomplished yet. The existence of antiferrotoroidic order has not yet been discussed. The practical value of ferrotoroidicity with respect to device applications is unclear and it is not known how to measure the toroidization of a ferrotoroidic state. These issues will be addressed in the following.

6.1. Switching and measuring the toroidization

As discussed in section 2.1.2 a space and time antisymmetric so-called toroidal field \mathbf{G} is required for introducing an energy difference between ferrotoroidic domains that allows one to switch them in a controlled way. According to (27) a field with $\nabla \times \mathbf{H} \neq 0$ is a toroidal field. Generating such a vortex field is difficult. A ring coil or an arrangement of current leads or permanent magnets may be used but this becomes unfeasible if a large amplitude or a low-temperature environment is required.

Alternatively, non-collinear homogeneous magnetic and electric fields are toroidal because $\mathbf{E} \times \mathbf{H}$ breaks the time-

and space-inversion symmetries. It may be argued that if two fields are used for switching the ferrotoroidic order parameter it represents a secondary rather than a primary ferroic state. However, it is still the toroidal field only that sets the order parameter; the fact that a combination of fields is used to generate it is not important. (Similarly, in a ferromagnetic material allowing the magnetoelectric effect $M_i = \beta_{ijk} E_j E_k$ a quadratic electric field can be used to orient the ferromagnetic order parameter without rendering ferromagnetism a secondary ferroic state!) Although the strength of the coupling between $\mathbf{E} \times \mathbf{H}$ and the toroidal field is not clear (see section 3), it is simpler to apply strong electric and magnetic fields rather than vortex fields, and a demonstration of ferrotoroidic switching may be accomplished in the near future.

Measurement of the toroidization faces similar problems. Although all the effects discussed in section 5 can in principle be used for quantifying the toroidization, the coupling constant connecting the toroidization to the magnetoelectric effect or to the gyration is not known. We anticipate that it will depend on the material under investigation so that only the relative values of the toroidization for one material at a time can be given. Measurement of the absolute value of a toroidization may be possible by using nanoscopic solenoids that pick up the magnetic vortex field and convert it into a measurable voltage in a capacitance.

6.2. Ferrotoroidicity and large magnetoelectric effects

A major advantage of ferrotoroidics is that they are intrinsically magnetoelectric so that they may be useful for manipulating magnetic properties by electric fields and vice versa. In that they resemble multiferroics with a coexistence of magnetic and ferroelectric order. However, whereas the unfavourable coexistence of two order parameters is required for breaking space and time reversal symmetries in a multiferroic, this is accomplished by a single order parameter in ferrotoroidics. Moreover, most of the magnetoelectric coefficients known at present are diagonal coefficients (α_{ii}). It is possible that the antisymmetric off-diagonal contributions coupling to the ferrotoroidic order parameter are intrinsically larger within the limits discussed in section 4.1. This is not refuted by the moderate values of the few known off-diagonal magnetoelectric coupling coefficients; these values might be due to compensation effects occurring in samples in a ferrotoroidic multidomain state.

6.3. Data storage applications

Ferrotoroidic materials may become useful for data storage applications in two ways. On the one hand, the possible existence of large magnetoelectric effects in ferrotoroidics may be used for magnetoelectric phase control in which a magnetic bit is written or read via electric fields. This can be realized by employing multilayer heterostructures with a ferrotoroidic magnetoelectric constituent next to a ferromagnetic constituent. Alternatively, the coexistence between ferrotoroidic and magnetic order in a single compound may be exploited to set the magnetization by an electric

field via the ferrotoroidically-induced magnetoelectric effect. On the other hand, the spontaneous toroidization itself may become the basis of binary data storage in which ferrotoroidic bits are written and read via the magnetoelectric effect. Admittedly, both options are still far from technical realization at present.

6.4. Ferrotoroidic versus antiferrotoroidic

One characteristic feature of a ferroic transition is uniform long-range ordering with respect to at least one macroscopic property. The macroscopic property (e.g. the magnetization \mathbf{M} of a ferromagnet) results from uniform alignment of a corresponding microscopic property (e.g. the magnetic dipole moment \mathbf{m}) for all unit cells of the parent phase: $\mathbf{M} = \sum_i \mathbf{m}_i$. If the alignment occurs in a cooperative but nonuniform way such that the associated macroscopic property is zero the corresponding transition is called *antiferroic*. For instance, antiparallel alignment of the magnetic moments in Cr_2O_3 leads to an antiferromagnetic state with $\mathbf{M} = 0$. At first glance, controlling the orientation of antiferroic domains is impossible because of the absence of a field-energy contribution as in (1). However, any antiferroic state also represents a ferroic state of higher order. For instance, the *antiferromagnetic* state in Cr_2O_3 is also *ferromagnetoelectric* in the terminology of section 2.1.1 so that domains can be oriented by simultaneous application of a magnetic and an electric field ($\mathbf{E} \parallel \mathbf{H}$ in Cr_2O_3 [54]). This approach allows one to classify even antiferroic states uniquely in terms of their field energy.

Symmetry-wise, an ordering is termed antiferroic if it breaks the same symmetries as a corresponding ferroic order but does not have the linear coupling (1) to external field. According to this definition, an antiferrotoroidic state must break both inversion and time reversal symmetry even though the total toroidal moment of such state is zero. These symmetry considerations can be used for classification of various types of domains observed in multiferroic hexagonal manganites. In YMnO_3 a coexistence of domains determined (i) by the ferroelectric order parameter P , (ii) by the antiferromagnetic order parameter ℓ and (iii) by the product $P\ell$ is observed and shown in figure 8(a). Independent domain structures are found for the order parameter P and for the somewhat artificial product $P\ell$, whereas the domains related to the order parameter ℓ are clearly not independent but determined by the other two domain structures. The interpretation becomes much more ‘physical’ by replacing $P\ell \rightarrow \tau$ and $\ell \rightarrow P\tau$ with τ as antiferrotoroidic order parameter since then the independent domain structures in figure 8(b) are those corresponding to the order parameters while the product state reasonably displays a constrained domain structure. As figure 8 shows, YMnO_3 can indeed be understood as being composed of three ferrotoroidic sublattices whose total toroidization cancels out.

The interpretation in terms of antiferrotoroidic domains is corroborated by SHG measurements. The ferroelectric and the antiferrotoroidic states yield SHG contributions while the product state ($\sim P\tau$) does not. The antiferrotoroidic SHG signal changes in the same way upon polarization reversal (spatial inversion) and upon spin reversal (temporal inversion)

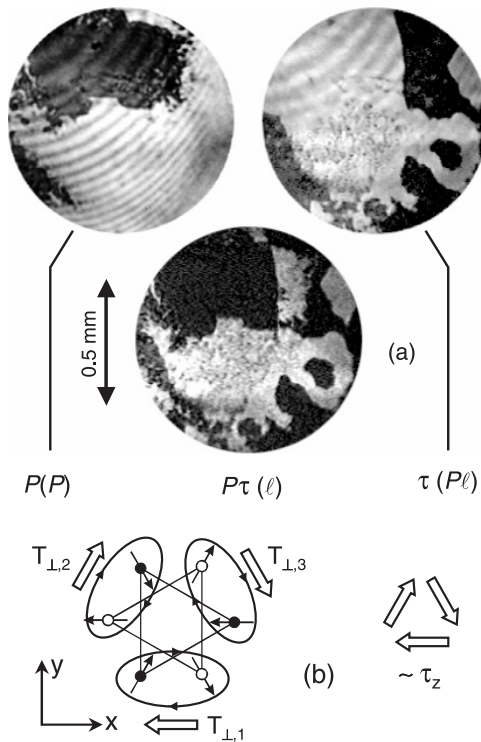


Figure 8. Possible existence of antiferrotoroidic domains in hexagonal YMnO_3 . (a) Coexistence of domain structures in a YMnO_3 sample at 6 K imaged with SHG light at 2.46 eV (see [48]). Labels refer to the coupling to the coupling of the SHG signal to the order parameters with former assignments given in brackets. P —ferroelectric, τ —antiferrotoroidic, ℓ —antiferromagnetic. (b) Graphical interpretation of the arrangement of Mn^{3+} spins in terms of compensated toroidal moments leading to antiferrotoroidicity. Filled and open circles refer to Mn^{3+} spins at $z = 0$ and $z = c/2$, respectively.

but it is left invariant by application of both. This corresponds precisely to the symmetry properties of a toroidic state.

7. Summary and outlook

7.1. State of the art

In this article we have shown that the concept of ferrotoroidicity as a long-range ordered arrangement of magnetic vortices is a compelling consequence of both a macroscopic as well as a microscopic classification of the crystalline state. Macroscopically, an expansion of the free energy leads to the existence of a primary ferroic state whose order parameter violates the space-inversion as well as the time reversal symmetry. A uniform alignment of toroidal moments has this property. Microscopically, toroidal moment emerges in the multipole expansion of the electrodynamic vector potential \mathbf{A} as a vector that changes sign upon both $\mathbf{r} \rightarrow -\mathbf{r}$ and $t \rightarrow -t$. We have shown how to apply the concept of toroidal moments to bulk periodic solids so that a well-defined value of the bulk toroidization is obtained: only differences in the toroidization of a system can be determined uniquely in analogy to the uniqueness of polarization differences only for ferroelectrics.

One of the most interesting properties of the ferrotoroidic state, directly following from its unusual symmetry, is its ability to show the linear magnetoelectric effect. We explained that any bulk toroidization leads to an antisymmetric magnetoelectric tensor $\alpha_{ij} = -\alpha_{ji}$, whereas the inverse is not mandatory. Thermodynamic stability imposes a stringent upper limit on the value of the magnetoelectric coupling coefficient. However, magnetoelectric effects can be drastically enhanced by proximity of ferroelectric and ferromagnetic transitions, where susceptibilities to uniform electric and magnetic field diverge and the magnetoelectric response is governed by non-equilibrium domain wall dynamics. In particular, when a spontaneous toroidization arises in a ferroelectric or ferromagnetic state, the magnetoelectric constant diverges at the critical temperature. Large magnetoelectric effects may also be found in magnetically frustrated systems, where spin orderings show strong sensitivity to external magnetic fields.

A review of experimental activities revealed a variety of techniques—many of them developed quite recently—that probe the simultaneous violation of spatial and temporal inversion symmetry. However, only two of them, namely the magnetoelectric effect and optical second harmonic generation have been applied for the actual observation of ferrotoroidic order. Future applications of ferrotoroidic materials and the possible existence of antiferrotoroidic order were discussed but much development is still required to advance these issues beyond speculation.

7.2. Unsolved problems

What are the important questions to be answered for further establishing the concept of ferrotoroidic order? From the point of view of theory, work on ferrotoroidic order to date has had a largely phenomenological character: magnetic classes allowing for the existence of spontaneous toroidal moment have been identified and Landau theory has been used to describe magnetoelectric anomalies and low-energy excitations close to critical points. However, the microscopic origins of ferrotoroidic ordering in solids remain largely unexplored. It has been hypothesized that such ordering can be induced by spontaneous currents circulating in certain types of excitonic insulators [6]. However, so far such materials have not been found and in all known ferrotoroidics the periodic arrays of magnetic vortices seem to be induced by a spin ordering. For spin-induced toroidal magnetism, it is not yet clear which lattice geometries and spin-exchange interactions are most favourable for ferrotoroidic ordering and how the magnetoelectric coupling in such materials can be increased. Can a macroscopically large toroidal moment be induced by a lattice instability in magnetically ordered states or by spontaneous charge currents generated in frustrated quantum spin systems (see appendix B)? In answering these questions, a fully first-principles method for calculating both spin and orbital contributions to the toroidal moment—analogue to the modern theories of polarization and orbital magnetization—would be very useful. While we believe that this is in principle possible, it will require extensive formal development and algorithmic implementation.

From the point of view of experiment a demonstration of controlled switching of the ferrotoroidic domains towards a single-domain state is most desirable. This will be attempted by subjecting a LiCoPO₄ sample to a toroidal field cycle. As mentioned, generation of a magnetic vortex field in a cryogenic environment is difficult. Therefore, as discussed in section 6.1, the toroidal field will be generated by crossed magnetic and electric fields applied below the ordering temperature of the compound. Electric field cycles at fixed magnetic field and magnetic field cycles at fixed electric field should have the same effect. The toroidization hysteresis will be determined by observing the field-dependent distribution of the ferrotoroidic domains by SHG. The field amplitude required for this purpose is not known because of the unknown value of the coupling constant between the toroidal field and the crossed magnetic and electric fields (see section 3). However, it was already observed that the ferrotoroidic domains are easily moved by small temperature cycles which points to a small coercive toroidal field [44].

‘Ferrotoroidic switching’ can also be used to search for novel mechanisms of ferrotoroidicity, as it makes it possible to differentiate between toroidal and antiferromagnetic orderings. Ideally, the toroidal field cycle will only affect the ferrotoroidic domain structure but leave any non-toroidal domain structure invariant. Indications that domains with different space–time symmetry can be manipulated independently were already reported in [44], but up to now on a passive basis, that is, in the absence of fields only. In addition, materials exhibiting a difference between antiferromagnetic and ferrotoroidic ordering temperatures should be sought.

Further corroboration of the ferrotoroidic state by some of the techniques discussed in section 5 is desirable. Here, resonant x-ray diffraction and (as yet not exploited) neutron diffraction seem to be most promising. More compounds displaying ferrotoroidic order, ideally accompanied by pronounced magnetoelectric effects, should be searched for. Such a quest should be supported by the present understanding of the microscopic origin of toroidal moments summarized in this article. Methods for directly measuring the value of the toroidization, based e.g. on the suggestions made in section 6.1, still need to be developed.

On a broader scope, further research on the topic of ferrotoroidic order will promote the development of a generalized concept of ferroic order. Figure 2 shows that with the addition of ferrotoroidicity to the set of primary ferroic forms of order each representation of the space–time parity group is now related to one primary ferroic state. However, three of these states correspond to an order parameter of rank-1 whereas the space and time symmetric ferroelastic state is parametrized by a rank-2 order parameter. It may be speculated that a yet undiscovered space and time symmetric primary ferroic state described by a vector may also exist and, moreover, other primary ferroic states related to an order parameter of second or even higher rank. For example, an electro-toroidal state with a vortex-like arrangement of electric (as opposed to magnetic) dipoles as proposed in [3] would constitute the ‘missing’ vector-like primary ferroic state. Electric vortices have already been observed. However,

thus far the vortex formation was always due to geometrical confinement and not related to long-range ordering.

Acknowledgments

NAS thanks the Division of Materials Research of the National Science Foundation (NSF) for financial support under grant number DMR-0605852, and the Miller Institute at UC Berkeley for their support through a Miller Research Professorship. MF thanks the SFB 608 of the DFG for financial support. This work was initiated during the research programme on Moments and Multiplets in Mott Materials at the Kavli Institute for Theoretical Physics at UC Santa Barbara under the NSF grant No. PHY05-51164.

Appendix A. Anapole moment

A toroidal moment was first discussed by Zel’dovich in the context of parity violation by weak interactions [55]. Since this moment was not like any conventional magnetic multipole known at that time it was named an *anapole moment*.

As discussed above, the toroidal moment \mathbf{t} changes sign under the symmetry operations $\mathbf{r} \rightarrow -\mathbf{r}$ and $t \rightarrow -t$. In particle-physics terminology, \mathbf{t} is thus a P -odd and T -odd vector. Since electromagnetic interactions, which are invariant under these two symmetry operations, are sufficient to describe physical properties of solids, the toroidal moment in condensed-matter systems appears as a result of *spontaneous* breaking of both spatial inversion and time reversal symmetry.

In particle physics the situation is somewhat different, because elementary particles and nuclei rotate and their eigenstates in the rest frame are eigenfunctions of the total spin. Then, according to the Wigner–Eckart theorem, the average toroidal moment of a particle has to be proportional to its average spin: $\langle \mathbf{t} \rangle \propto \langle \mathbf{S} \rangle$. Since spin is P -even and T -odd, while $\langle \mathbf{t} \rangle$ is P -odd and T -odd, a nonzero toroidal moment \mathbf{t} of a particle requires explicit parity-breaking terms in the Hamiltonian, originating from weak interactions. The toroidal moment of a nucleus induces the P -even electromagnetic vector potential $\mathbf{A} = 4\pi \mathbf{t} \delta(\mathbf{R})$ (see (9)), which acts on atomic electrons.

Observation of the nuclear toroidal moment at $r = 0$ is possible via its contact interaction with the orbital current of the much more extended electron cloud described by $H_{\text{int}} = -\frac{4\pi}{c} \mathbf{j}_e(0) \cdot \mathbf{t}$, where $\mathbf{j}_e(0) = -\frac{e\hbar}{2im} (\psi^\dagger(0) \nabla \psi(0) - \text{h.c.})$. Since $\psi(0)$ is nonzero for s orbitals while the derivative of ψ at $r = 0$ is nonzero for p orbitals, the transfer of the parity-breaking nuclear toroidal moment to the electrons results in the mixing of s and p electron states. For Cs atoms the admixture of the p wavefunction to the $6s$ and $7s$ state was evidenced by observation of an electric dipole transition between the two states [56].

Appendix B. Persistent currents in Mott insulators and quantum toroidal states

So far we discussed toroidal moments induced by classical spin ordering. Here we show that the ground state degeneracy

in frustrated quantum spin systems can result in states with spontaneously broken space-inversion and time reversal symmetry that carry a toroidal moment.

Consider an isolated equilateral triangle in the xy plane formed by three $S = 1/2$ spins with antiferromagnetic Heisenberg interactions. Its ground state is four-fold degenerate and has the total spin $S = 1/2$. The degenerate ground states can be labelled by z -projection of the total spin, $S_z = \pm 1/2$ and by the ‘scalar chirality’ [57], $\chi = \pm 1$:

$$|\chi, \uparrow\rangle = +\frac{1}{\sqrt{3}} \left(|\downarrow\uparrow\uparrow\rangle + e^{i\chi\frac{2\pi}{3}} |\uparrow\downarrow\uparrow\rangle + e^{i\chi\frac{4\pi}{3}} |\uparrow\uparrow\downarrow\rangle \right),$$

$$|\chi, \downarrow\rangle = -\frac{1}{\sqrt{3}} \left(|\uparrow\downarrow\downarrow\rangle + e^{i\chi\frac{2\pi}{3}} |\downarrow\uparrow\downarrow\rangle + e^{i\chi\frac{4\pi}{3}} |\downarrow\downarrow\uparrow\rangle \right)$$
(B.1)

The operator of scalar spin chirality,

$$\hat{\chi} = \frac{4}{\sqrt{3}} \mathbf{S}_1 \cdot (\mathbf{S}_2 \times \mathbf{S}_3),$$
(B.2)

describes the direction of an orbital current circulating in the triangle. This persistent charge current results from the fact that the amplitudes of clockwise and anti-clockwise permutations of three electrons in the triangle are different in chiral states. Such states carry an orbital magnetic moment coupled to the magnetic field [59]. These four degenerate states are also eigenfunctions of the ‘vector chirality’ operator, \hat{V}_z : $\hat{V}_z|\chi, S_z\rangle = 2S_z\chi|\chi, S_z\rangle$, where the vector chirality operator is defined by [58]

$$\mathbf{V} = \frac{2}{\sqrt{3}} [\mathbf{S}_1 \times \mathbf{S}_2 + \mathbf{S}_2 \times \mathbf{S}_3 + \mathbf{S}_3 \times \mathbf{S}_1].$$
(B.3)

The average value of the pseudoscalar operator a and the toroidal moment t_z , defined by (23) and (24), over chiral states is zero, which is clear already from the fact that the chiralities χ and V_z are even under the xy mirror transformation, while a and t_z are odd. However, the linear superpositions of chiral states with real coefficients,

$$|\pm\rangle_a = \frac{1}{\sqrt{2}} (|+, \downarrow\rangle \mp |-, \uparrow\rangle),$$
(B.4)

are eigenstates of a with the eigenvalues $\pm \frac{2l_0g\mu_B}{3\sqrt{3}}$, where l_0 is the length of the triangle side, while the superpositions with complex coefficients

$$|\pm\rangle_t = \frac{1}{\sqrt{2}} (|+, \downarrow\rangle \pm i|-, \uparrow\rangle),$$
(B.5)

are eigenstates of t_z with the eigenvalues $\pm \frac{l_0g\mu_B}{\sqrt{3}}$. Thus, frustrated triangular antiferromagnets can in principle show magnetoelectric effect of quantum spin origin. It is not clear, however, whether realistic interactions between spins of different triangles can favour such ‘quantum magnetoelectric’ states.

References

[1] Wilczek F 1990 *Fractional Statistics and Anyon Superconductivity* (Singapore: World Scientific)

[2] Borzi R A, Grigera S A, Farrell J, Perry R S, Lister S J S, Lee S L, Tennant D A, Maeno Y and Mackenzie A P 2007 *Science* **315** 214

[3] Dubovik V M and Tugushev V V 1990 *Phys. Rep.* **187** 145

[4] Fiebig M 2005 *J. Appl. Phys.* **D** **38** R123

[5] Ederer C and Spaldin N A 2007 *Phys. Rev. B* **76** 214404

[6] Gorbatshev A A and Kopaev Y V 1994 *Ferroelectrics* **161** 321

[7] Halperin B I, March-Russel J and Wilczek F 1989 *Phys. Rev. B* **40** 8726

[8] Wadhawan V K 2000 *Introduction to Ferroic Materials* (New York: Gordon and Breach)

[9] Landau L D and Lifshitz E M 1980 *The Classical Theory of Fields* (Amsterdam: Elsevier) pp 110–3

[10] Popov Yu F, Kadomtseva A M, Vorobev G P, Timofeeva V A, Ustinin D M, Zvezdin A K and Tegeranchi M M 1998 *JETP* **87** 146

[11] Schmid H 2001 *Ferroelectrics* **252** 41

[12] Vanderbilt D and King-Smith R D 1993 *Phys. Rev. B* **48** 4442

[13] Arima T, Jung J H, Matsubara M, Kubota M, He J P, Kaneko Y and Tokura Y 2005 *J. Phys. Soc. Japan* **74** 1419

[14] Sawada K and Nagaosa N 2005 *Phys. Rev. Lett.* **95** 237402

[15] Kida N, Yamada H, Sato H, Arima T, Kawasaki M, Akoh H and Tokura Y 2007 *Phys. Rev. Lett.* **99** 197404

[16] Thiel S, Hammerl G, Schmehl A, Schneider C W and Mannhart J 2006 *Science* **313** 1942

[17] Nakagawa N, Hwang H Y and Muller D A 2006 *Nat. Mater.* **5** 204

[18] Yamasaki Y, Miyasaka S, Kaneko Y, He J-P, Arima T and Tokura Y 2006 *Phys. Rev. Lett.* **96** 207204

[19] Landau L D and Lifshitz E M 1984 *Electrodynamics of Continuous Media* (Oxford: Pergamon)

[20] Cheong S-W and Mostovoy M 2007 *Nat. Mater.* **6** 13

[21] Kimura T 2007 *Annu. Rev. Mater. Res.* **37** 387

[22] Siratori K, Akimitsu J, Kita E and Nishi M 1980 *J. Phys. Soc. Japan* **48** 1111

[23] Siratori K and Kita E 1980 *J. Phys. Soc. Japan* **48** 1443

[24] O’Dell T H 1966 *Phil. Mag.* **13** 961

[25] Brown W F, Hornreich R M and Shtrikman S 1968 *Phys. Rev.* **168** 574

[26] Ramirez A P 1994 *Annu. Rev. Mater. Res.* **24** 453

[27] Nelmes R J 1974 *J. Phys. C: Solid State Phys.* **7** 3840

[28] Sannikov D G 1997 *JETP* **84** 293

[29] Sannikov D G 1998 *Ferroelectrics* **219** 177

[30] Gehring G A 1994 *Ferroelectrics* **161** 275

[31] Katsura H, Nagaosa N and Balatsky A V 2005 *Phys. Rev. Lett.* **95** 057205

[32] Sergienko I A and Dagotto E 2006 *Phys. Rev. B* **73** 094434

[33] Sergienko I A, Sen C and Dagotto E 2006 *Phys. Rev. Lett.* **97** 227204

[34] Goodenough J 1963 *Magnetism and the Chemical Bond* (New York: Wiley)

[35] Delaney K, Mostovoy M and Spaldin N A 2008 at press

[36] Sannikov D E 1997 *JETP* **84** 293

[37] Popov Yu F, Kadomtseva A M, Vorobev G P, Timofeeva V A and Ustinin D M 1998 *JETP* **87** 146

[38] Popov Yu F, Kadomtseva A M, Belov D V, Vorobev G P and Zvezdin A K 1999 *JETP Lett.* **69** 330

[39] Goulon J, Rogalev A, Goulon-Ginet C, Benayoun G, Paolasini L, Brouder C, Malgrange C and Metcalf P A 2000 *Phys. Rev. Lett.* **85** 4385

[40] Goulon J, Rogalev A, Wilhelm F, Goulon-Ginet C, Carra P, Cabaret D and Brouder C 2002 *Phys. Rev. Lett.* **88** 237401

[41] Kubota M, Arima T, Kaneko Y, He J P, Yu X Z and Tokura Y 2004 *Phys. Rev. Lett.* **92** 137401

[42] Rikken G L J A and Raupach E 1997 *Nature* **390** 493

[43] Krichevtsov B B, Pavlov V V, Pisarev R V and Gridnev V N 1993 *J. Phys.: Condens. Matter* **5** 8233

[44] Van Aken B B, Rivera J P, Schmid H and Fiebig M 2007 *Nature* **449** 702

- [45] Shen Y R 2002 *The Principles of Nonlinear Optics* (New York: Wiley)
- [46] Pershan P S 1963 *Phys. Rev.* **130** 919
- [47] Lottermoser Th, Lonkai T, Amman U, Hohlwein D, Ihringer J and Fiebig M 2004 *Nature* **430** 541
- [48] Fiebig M, Lottermoser Th, Fröhlich D, Goltsev A V and Pisarev R V 2002 *Nature* **419** 818
- [49] Fiebig M, Fröhlich D, Krichevtsov B B and Pisarev R V 1994 *Phys. Rev. Lett.* **73** 2127
- [50] Fiebig M, Fröhlich D, Sluyterman G and Pisarev R V 1995 *Appl. Phys. Lett.* **66** 2906
- [51] Fiebig M, Fröhlich D, Kohn K, Leute S, Lottermoser Th, Pavlov V V and Pisarev R V 2000 *Phys. Rev. Lett.* **84** 5620
- [52] Fiebig M, Fröhlich D, Lottermoser Th and Kallenbach S 2004 *Opt. Lett.* **29** 41
- [53] Matsuno J, Lottermoser Th, Arima T, Kawasaki M and Tokura Y 2007 *Phys. Rev. B* **75** 180403
- [54] Krichevtsov B B, Pavlov V V and Pisarev R V 1988 *Sov. Phys.—JETP* **67** 378
- [55] Zel'dovich Ya B 1958 *Sov. Phys.—JETP* **6** 1184
- [56] Wood C S, Bennett S C, Cho D, Masterson B P, Roberts J L, Tanner C E and Wieman C E 1997 *Science* **275** 1759
- [57] Wen X G, Wilczek F and Zee A 1989 *Phys. Rev. B* **39** 11413
- [58] Kawamura H 1998 *J. Phys.: Condens. Matter* **10** 4707
- [59] Bulaevskii L N, Batista C D, Mostovoy M and Khomskii D 2008 *Phys. Rev. B* at press (*preprint* 0709.0575)